Xenoestrogens Ethinyl Estradiol and Zearalenone Cause Precocious Puberty in Female Rats via Central Kisspeptin Signaling

Rókus Kriszt, Zsuzsanna Winkler, Ágnes Polyák, Dániel Kuti, Csilla Molnár, Erik Hrabovszky, Imre Kalló, Zsuzsanna Szőke, Szilamér Ferenczi,* and Krisztina J. Kovács*

Laboratory of Molecular Neuroendocrinology (R.K., Z.W., A.P., D.K., S.F., K.J.K.) and Department of Endocrine Neurobiology (C.M., E.H., I.K.), Institute of Experimental Medicine, and Faculty of Information Technology and Bionics (A.P.), Roska ~~Tamás~~ Doctoral School of Sciences and Technology, Pázmány Péter Catholic University, Budapest H-1083, Hungary; Soft Flow Hungary Research and Development Ltd (Z.S.), Pécs, Hungary; János Szentágothai Doctoral School of Neurosciences (R.K., Z.W., D.K.), Semmelweis University, H-1085 Budapest, Hungary

Xenoestrogens from synthetic or natural origin represent an increasing risk of disrupted endocrine functions including the physiological activity of the hypothalamo-pituitary-gonad axis. Ethinyl estradiol (EE2) is a synthetic estrogen used in contraceptive pills, whereas zearalenone (ZEA) is a natural mycoestrogen found with increasing prevalence in various cereal crops. Both EE2 and ZEA are agonists of estrogen receptor-α and accelerate puberty. However, the neuroendocrine mechanisms that are responsible for this effect remain unknown. Immature female Wistar rats were treated with EE2 (10 μg/kg), ZEA (10 mg/kg), or vehicle for 10 days starting from postnatal day 18. As a marker of puberty, the vaginal opening was recorded and neuropeptide and related transcription factor mRNA levels were measured by quantitative real time PCR and in situ hybridization histochemistry. Both ZEA and EE2 accelerated the vaginal opening, increased the uterine weight and the number of antral follicles in the ovary, and resulted in the increased central expression of *gnrh*. These changes occurred in parallel with an earlier increase of *kiss1* mRNA in the anteroventral and rostral periventricular hypothalamus and an increased kisspeptin (KP) fiber density and KP-GnRH appositions in the preoptic area. These changes are compatible with a mechanism in which xenoestrogens overstimulate the developmentally unprepared reproductive system, which results in an advanced vaginal opening and an enlargement of the uterus at the periphery. Within the hypothalamus, ZEA and EE2 directly activate anteroventral and periventricular KP neurons to stimulate GnRH mRNA. However, GnRH and gonadotropin release and ovulation are disrupted due to xenoestrogen-mediated inhibitory KP signaling in the arcuate nucleus. **(*Endocrinology* 156: 0000–0000, 2015)**

Xenoestrogens are synthetic or naturally occurring estrogen mimetic compounds that have been implicated in precocious puberty and a variety of other reproductive anomalies. However, their neuroendocrine mechanisms of actions are not fully understood.

Zearalenone (ZEA) is an estrogenic mycotoxin produced by several *Fusarium* species (1). ZEA is found worldwide in livestock feed and human food made from cereal crops such as maize, barley, oats, and rice (2). In food, ZEA contamination may reach a level that disrupts endocrine/reproductive functions (3).

The estrogenic effect of ZEA and its metabolites, α- and β-zearalenol, has been verified in silico (4, 5), in vitro (6), and in vivo (7, 8). Due to similarities in the molecular

ISSN Print 0013-7227 ISSN Online 1945-7170
Printed in USA

Received April 13, 2015. Accepted July 31, 2015.

* S.F. and K.J.K. contributed equally to this work.

Abbreviations: ARC, arcuate nucleus; AVPV, anteroventral periventricular nucleus; bw, body weight; cRNA, complementary RNA; DTT, dithiothreitol; EE2, ethinyl estradiol; EIA, enzyme immunoassay; ER, estrogen receptor; GPR54, G protein-coupled receptor 54; HPG, hypothalamo-pituitary-gonad; KP, kisspeptin; MKRN 3, makorin 3; PeV, periventricular; PND, postnatal day; ~~RING, really interesting new gene;~~ SSC, saline sodium citrate; ZEA, zearalenone.

structure of ZEA and 17β-estradiol, ZEA has the capability to bind to the ligand-binding pocket of the estrogen receptor (ER) and stabilize at least one of the functionally active conformations of the receptor's ligand binding domain (5). ZEA preferentially activates ERα and displays partial antagonist activity on ERβ, especially at high concentrations (9, 10).

Depending on the developmental timing of mycotoxin exposure, ZEA has multiple adverse effects on female reproduction (11) including enlargement of the uterus (7, 8), persistent anovulatory cycles (12, 13), decreased fertility, and defective embryonic implantation and development (14).

It has been repeatedly shown that ZEA administration accelerates the puberty onset in mice (13, 15) and rats (8) but not in gilts (11, 12, 16).

Sporadic epidemics of precocious puberty in human females were attributed to exposure of anabolic estrogens in animal foods such as ZEA in Italy (17), Puerto Rico (18, 19), and Hungary (20). However, the neuroendocrine mechanism through which estrogenic mycotoxins accelerate puberty onset remains to be elucidated.

Ethinyl estradiol (EE2) is the major estrogenic component of contraceptive pills, which are often taken at peripubertal ages. EE2 is also prescribed to alleviate menopausal symptoms, used as palliative therapy in malignant tumors of breast and prostate cancer, and also applied as steroid substitution to girls with Turner syndrome. Unintended EE2 exposure may also originate from the environment, in which significant amounts of EE2 have been detected due to the urine and feces of women taking the contraceptive pill. An additional load may originate from livestock and aquaculture (21, 22). EE2 and ZEA are both ERα ligands. Previous in vivo studies have shown that EE2 and ZEA elicit similar effects on the timing of puberty, although ZEA has a lower efficacy and a 1000-fold lower potency than EE2 (6, 23). Increasing evidence indicating that exposure to different estrogenic compounds results in compound-specific effects on morphological, histological, and molecular level (24, 25) led us to study and compare neuroendocrine mechanisms that are responsible for advanced puberty in rats treated with EE2 and ZEA.

Kisspeptin (KP) and its receptor, G protein-coupled receptor 54 (GPR54) (kisspeptin-1 receptor) have been implicated in initiation of puberty and regulation of the hypothalamo-pituitary-gonad (HPG) axis through GnRH synthesis and release (26–29). KP is synthesized by two distinct groups of hypothalamic neurons in the anteroventral periventricular (AVPV) and arcuate (ARC) nuclei, respectively (30, 31). KP is a potent GnRH secretagogue, results in depolarization of GnRH neurons, and advances puberty in mice (28). By contrast, mutations of the *gpr54* gene are associated with impaired sexual maturation in mice and humans (32, 33). Furthermore, GnRH-specific ~~gpr54~~ knockout results in delayed puberty onset, abnormal estrus cycles, and infertility (34, 35).

Most KP neurons express ERα, which plays a fundamental role in mediation of steroid feedback on the HPG axis (36–38). The two KP neuron populations display differential responsiveness to estrogens because *kiss1* expression is stimulated by 17β-estradiol in the AVPV but inhibited in the ARC (39, 40). Furthermore, studies on mice with conditional knockout of the ERα gene from kisspeptin neurons revealed that estrogen-responsive KP cells in the arcuate nucleus restrain the HPG axis and delay puberty onset in juvenile animals, whereas subsequent ER-dependent activation of GnRH neurons depends on AVPV KP input, which accelerates gonadal, hormonal, and sexual maturation during puberty (41). Recent findings suggest that puberty occurs when *kiss1* in the ARC is relieved from the suppression mediated by the polycomb group of transcription silencing complexes before puberty (42). Furthermore, the expression of makorin3 (*mkrn3*), which encodes a transcriptional suppressor protein with ~~a really interesting new gene (RING)~~ finger domain, also declines in the mouse hypothalamus before puberty (43).

There is increasing evidence for a correlation between body levels of estrogenic endocrine disruptor compounds and precocious puberty in girls. For instance, urinary bisphenol levels were significantly higher in girls with idiopathic central precocious puberty (44). Recently the association of phthalate exposure, kisspeptin plasma levels, and precocious puberty has been revealed (45). We hypothesized that the endocrine disruptor effect of the xenoestrogens ZEA and EE2 is mediated through kisspeptin-kisspeptin-1 receptor signaling in the hypothalamus. To address this issue, female prepubertal Wistar rats were exposed to ZEA, (an estrogenic mycotoxin) or EE2, (a prototype of estrogenic disruptor compounds), and the physiological and hormonal responses were analyzed together with changes in kisspeptinergic signaling on GnRH neurons. Both EE2 and ZEA advanced puberty onset in females. This was accompanied by selective increase of *kiss1* and *gnrh* mRNA expression in the anterior hypothalamus, without noticeable changes of kisspeptin signaling in the ARC. These results identify kisspeptin-GPR54 signaling as a central target of the endocrine disruptor effect of EE2 and the ZEA.

Materials and Methods

Animals

Female Wistar rats (n = 40) from the colony bred at the Institute of Experimental Medicine (Budapest, Hungary) were

doi: 10.1210/en.2015-1330

used. Animals were kept at the minimal disease (MD) level of the institute's animal facility under standard conditions (temperature 22°C ± 3°C; relative humidity 30%–70%; lighting 12 h light, 12 h dark cycle; lights on at 7:00 AM). Animals had free access to phytoestrogen-free rodent diet (Harlan Teklad Global Diets) and tap water. Rats were weaned, weighed, and randomly allocated to treatment groups at postnatal day (PND) 18. All procedures were conducted in accordance with the guidelines set by the European Communities Council Directive (86/609 EEC) and approved by the Institutional Animal Care and Use Committee of the Institute of Experimental Medicine (permit numbers PEI/001/35-4/2013 and PEI/ 001/29-4/2013).

Treatment and processing

Rats were treated with EE2 (Sigma; 10 μg/kg body weight) or ZEA (Sigma; 10 mg/kg body weight [bw]) for 10 consecutive days, starting at PND 18 according to the protocol used for the immature rat uterotrophic assay developed and validated by the Organisation for Economic Co-operation and Development (protocol number 440, http://www.epa.gov/endo/pubs/uterotrophic_oecd_guideline.pdf). The dose of the ZEA was based on our previous study (8), whereas the dose of EE2 was selected in a pilot uterotrophic assay (Supplemental Figure 1). EE2 and ZEA were dissolved first in alcohol and then diluted in olive oil at a ratio of 1% ethanol and 99% oil. The vehicle was also prepared with the same ratio. Drugs and vehicle were administered daily by oral gavage (1 mL/kg bw), between 9:00 and 11:00 AM. For each animal, individual doses were calculated daily, after measurement of the body weight. Based on the dose-response studies, in the main experiment, the following groups were used: 10 μg/kg bw EE2 (n = 14), 10 mg/kg bw ZEA (n = 11), and the vehicle oil (control, n = 15). Rats were randomly assigned to treatment groups. Animals were housed in groups of four to five per cage during treatment, and the sequence of the treatments varied day by day. The weight of animals and food and water consumption were measured, and the vaginal opening was examined daily, before gavage.

On PND 28, vaginal smears were taken, and then the rats were killed by decapitation, and trunk blood was collected for hormone measurement. The brain was rapidly removed from the skull, placed into acrylic coronal matrix, and dissected to isolate an AVPV/preoptic area (POA)-enriched region and an ARC-enriched region (see Figure 3). Viewing from the ventral surface of the brain, a series of three cuts in the coronal plane were made using a sterile razor blade: the first cut was placed 2 mm in front of the optic chiasm, the second one at the apex of the pituitary stalk, and the third one at the rostral margin of the mammillary bodies. This sectioning resulted in two hypothalamic slabs that were placed flat facing to the plane of the second cut. AVPV/POA regions were dissected from the first slab by two sagittal cuts 2 mm from the midline and one horizontal cut just above the third ventricle. ARC-enriched samples were prepared from the second slab by placing two sagittal cuts on either side of the optic tract and a horizontal cut through the middle of the third ventricle. To control the amount of tissue dissected per rats, and thus entering the reverse transcription reaction, hypothalamic tissue samples were weighed. No significant differences in the weight of hypothalamic tissue samples were observed between comparable experimental groups. Dissected tissue samples were immediately frozen on dry ice and stored at −70°C until assay.

At autopsy, ovaries and the uterus were also removed, weighed, and immersion fixed in 10% buffered formalin. Tissue samples were embedded in paraffin, sectioned (10 μm), and stained with hematoxylin-eosin. All microscopic analyses were performed blind to the identification of any group.

RNA isolation and quantitative RT-PCR

For total RNA isolation, hypothalamic blocks were homogenized in 500 μL TRI reagent (Ambion). Total RNA was isolated using a total RNA minikit (Geneaid) according to the manufacturer's instructions. To eliminate genomic DNA contamination, deoxyribonuclease I treatment was introduced (1 U per reaction, reaction volume 50 μL ribonuclease-free deoxyribonuclease I; Fermentas). Sample quality control and the quantitative analysis were carried out by NanoDrop (Thermo Scientific). cDNA synthesis was performed with the high-capacity cDNA reverse transcription kit (Life Technologies) according to the manufacturer's instructions.

The chosen primer sequences used for the comparative cycle threshold experiments were verified with the Primer Express 3.0 program. The sequences were as follows: *gnrh*, forward, CCCCAAACTGATGGCCGCTGTT, reverse, AGGGCGCAACCCATAGGACCA; *kiss1*, forward, CACCTGTGGTGAACCCTGAAC, reverse, CAGGCTTGCTCTCTGCATACC; *gpr54*, forward, TGCAGACCGTCACCAATTTC, reverse, TGAAGGGTACGCAGCACAGA; *gapdh*, forward, ACAGCCGCATCTTCTTGTGC, reverse, GCCTCACCCCATTTGATGTT; *nkb*, forward, CTAGCGTGGGACCGAAGGA, reverse, GCCCATAAGTCCCACAAAGAAGT; *dyn*, forward, GAATCTGAGCTACTGGGCACTGA, reverse, TTTCTCAAGTCCTCCTCGTTGAA; *th*, forward, AGTACAAGCACGGTGAACCA, reverse, GATGCTGTCCTCTCGGTAGC; *eap1*, forward, CTACGAGGTGCGCTTCAAGA, reverse, CTTAGAGACCGCGTCGAAGG; *ttf1 (nkx2)*, forward, CGGGCAAGATGTAGGCTTCTA, reverse, CATGATTCGGCGTCGGCTTAAC; *mkrn3*, forward, GCTCCGCAATTCAAGCACAA, reverse, AGCGTGCCTCTAACACTGTC; *cux1*, forward, GAAAGGCCGAGAACCCTTCA, reverse, TGGTCCTTGTTGTTGCCCTT; *eed*, forward, GAACAGCAACCCGGACCTCTCG, reverse, TTCCCTTTCCCCAGCTTTTCCTTC; *cbx7*, forward, GACGCCCATGCTCCCCTCAAGT, reverse, CCTCACCCAAGCCCCAAGAAACAC; *erα*, forward, CCGCCTTCTACAGGTCCAAT, reverse, GAAAGCCTTGCAGCCTTCAC; and *erβ*, forward, GTTGTGCCAGCCCTGTTACTAGTC, reverse, GGTACACTGATTCGTGGCTGGACAGATATA.

The primers (Invitrogen) were used in a real-time PCR with a Fast EvaGreen quantitative PCR master mix (Biotium) on an ABI StepOnePlus instrument (Applied Biosystems). The gene expression was analyzed using the ABI StepOne 2.1 program (Applied Biosystems). The amplicons were tested by melt curve analysis on an ABI StepOnePlus instrument (Applied Biosystems). Experiments were normalized to *gapdh* expression.

Perfusion and tissue processing for in situ hybridization histochemistry and immunocytochemistry

Another set of vehicle-, ZEA-, and EE2-treated rats (n = 16) was deeply anesthetized on PND 28 with pentobarbital (100 mg/kg, ip) and perfused through the ascending aorta with saline followed by ice-cold fixative (4% paraformaldehyde in 0.1M Borate buffer [pH 8]). Brains were postfixed in the fixative for 3

AQ: 10 hours and then placed in 0.1 M potassium PBS containing 10% sucrose overnight. A series of 30-μm frontal sections were cut on a freezing microtome, collected in a cryoprotectant, and stored at −20°C until processing.

In situ hybridization histochemistry

AQ: 11 Antisense complementary RNA (cRNA) probes labeled by ^{35}S-uridine triphosphate (DuPont NEN) were used throughout. The kisspeptin probe was transcribed from a 411-bp mouse cDNA template (bases 76–486 of AF472576) subcloned into pGEMTEasy. The plasmid was linearized by *Sac*1 and used as template for in vitro RNA transcription using T7 RNA polymerase.

The probe for GPR54 in situ hybridization histochemistry was produced in our laboratory using rat hypothalamic cDNA as a template to generate a *gpr54*-specific PCR fragment. The PCR was carried out using *gpr54* forward and T7 *gpr54* antisense primers. The amplicon was visualized by gel electrophoresis AQ: 12 (1.8% agarose gel, 0.5 × Tris-borate EDTA buffer), and the *gpr54*-specific PCR product (473 bp) was isolated from the gel (gel/PCR DNA fragment extraction kit; Genaid). This fragment (10 ng) was served as a template to a second PCR to increase the specificity of the *gpr54* amplicon. The second PCR was carried out using T7 and *gpr54* forward primers, and the PCR product was visualized and isolated as above. Details of the PCRs and primer sequences are described in the Supplemental Methods. The amplicon (50 ng) served as a template for in vitro radionu- AQ: 13 clide (^{35}S-uridine ~~5~~-triphosphate; DuPont NEN)-labeled cRNA probe synthesis using T7 RNA polymerase. The specificity of the designed primers was verified by Primer Blast software.

Hybridization and autoradiographic procedures were modified following those of Simmons et al (46). Tissue sections were mounted onto SuperFrost Ultra Plus slides (Menzer-Glazer Braunschweig) postfixed with 4% paraformaldehyde, digested with Proteinase K (10 μg/mL in 50 mM Tris [pH 8] and 5 mM EDTA [pH 8] at 37°C for 10 min), acetylated (0.25% acetic anhydride in 0.1 M triethanolamine [pH 8]), and dehydrated. Hybridization mixture (50% formamide, 0.3 M NaCl, 10 mM Tris [pH 8], 2 mM EDTA, 1× Denhardt's, 10% dextran sulfate, AQ: 14 0.5 mg/mL yeast tRNA, and 10 mM dithiothreitol [DTT]) was pipetted onto the slides (100 μL, containing probe at 10^7 dpm/mL) and hybridized overnight at 56°C. Sections were then rinsed AQ: 15 in 4× saline sodium citrate [SSC] (1× SSC: 0.15 M NaCl and 15 mM trisodium citrate buffer, [pH 7]), digested with ribonuclease A (20 μg/mL in Tris-EDTA buffer with 0.5 M NaCl at 37°C for 30 min), gradually desalted in 2× SSC-1× SSC-0.5× SSC all with 1 mM DTT for 5 minutes each, and washed in 0.1× SSC with 1 mM DTT at 65°C–75°C for 30 minutes and dehydrated in alcohols. Slides were exposed to Phosphoimager image plates for AQ: 16 24–48 hours and then dipped in ~~nitroblue tetrazolium salt~~ nuclear emulsion (Kodak) and exposed for 2–3 weeks, developed in D-19 developer, and lightly counterstained with cresyl violet. Densitometric analysis of the in situ hybridization histochemistry was performed using the advanced Image Data Analyzer (AIDA version 3.1) software on scanned images obtained by the BASReader program (Raytest Isotopenmessegerate GmbH). Anatomical regions of interest were identified using a rat brain atlas. The density measurement was corrected by subtraction of a background value obtained from a neighboring nonhybridized tissue area from the same section.

Double immunofluorescence for GnRH and kisspeptin immunoreactivity

To evaluate changes in KP fiber density and kisspeptinergic inputs to GnRH neurons, double-labeling immunofluorescence was performed. After blocking in 2% normal goat and donkey serum, free-floating sections were incubated in a mixture of guinea pig anti-GnRH (number 1018 Hrabovszky, 1:3000 [47]) and rabbit anti-KP (number 566, Caraty, 1:10 000 [48]) overnight at 4°C. The antigens were then visualized by biotinylated goat antiguinea pig IgG (Vector Labs; dilution 1:500) for 1 hour followed by streptavidin ALEXA 350 (Molecular Probes; 1:500) and donkey antirabbit ALEXA 488 (Molecular Probes; 1:500) for 3 hours. After PBS washing, the sections were mounted onto chrome-alum gelatin-coated slides and coverslipped with Pro-Long Gold antifade reagent (Life Technologies).

Confocal microscopic analysis

Confocal imaging was performed on Olympus FluoView FV1000 (Olympus) laser-scanning confocal microscope using ×100/1.45 oil objective. All image acquisition and quantification was performed by an individual blind to the treatment conditions. Images were consistently collected at, but not past, the threshold of overexposure to standardize analysis parameters across image stacks. KP fiber projections to GnRH neurons were evaluated at the rostral POA by using z-stack imaging. Three-dimensional image analysis was carried out by using Imaris software (Bitplane). From each animal, nine GnRH neurons were selected in the double-immunostained (GnRH and KP) material using the following criteria: 1) the cell had definitive GnRH immunoreactivity, 2) the total plane of the soma was visible within the z-stack, 3) had a defined nucleus, and 4) sufficiently separated from other cells to clearly identify kisspeptin fiber appositions. The GnRH neurons were identified by slowly scrolling through the z-plane. To quantify the number of GnRH/KP appositions, we counted the total number of immunoreactive boutons in apposition to the soma through the complete z axis of each of the nine cells. These appositions were defined by visualizing no visible space between KP-immunoreactive profiles and the GnRH cell membrane.

GnRH/KP double-stained hypothalamic sections have been used to quantify KP fiber density in the preoptic area. The region of interest has been selected by revealing GnRH-immunoreactive cells, and the density of KP-immunoreactive fibers were analyzed after thresholding in ImageJ software (National Institutes of Health, Bethesda, Maryland). In this analysis the data represent the area occupied by immunolabeled fibers as a proportion of the total region of interest area but not the specific number of fibers.

Hormone measurement

After decapitation, trunk blood was collected into ice-cold EDTA-containing tubes, centrifuged, and plasma samples were then stored at −20°C until assay. Plasma hormone levels were measured by enzyme immunoassay (EIA) kits obtained from NovaTec Immunodiagnostica GmBH, according to the manufacturer's instructions. 17-β-Estradiol EIA kit (catalog number DNOV003; assay range 0–2000 pg/mL; sensitivity 5 pg/mL; accuracy 96.5% ± 3.1%; intra- and interassay coefficients of variations are 3.2% and 5.4%, respectively). The assay showed less than 0.001% cross-reactivity with ZEA. The lowest detectable concentrations of FSH (catalog number DNOV031) and LH

doi: 10.1210/en.2015-1330

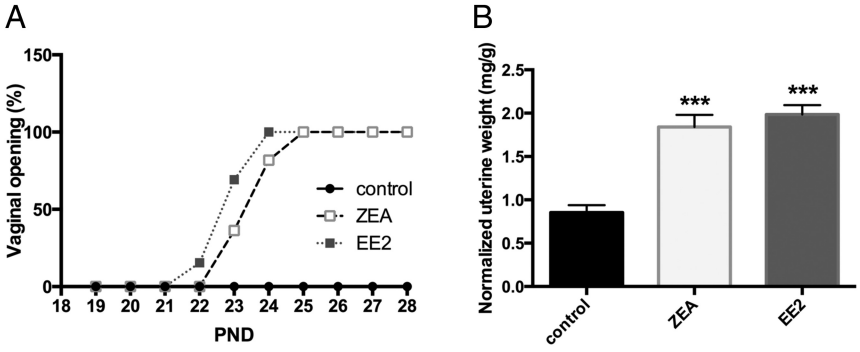

Figure 1. Effect of xenoestrogens on the vaginal opening and uterus weig. A, Percentage of rats displaying a vaginal opening after ZEA or EE2 treatment. None of the vehicle-treated control animals had a vaginal opening until the end of the experiment (PND 28). B, The mean ± SEM values of the uterine weights normalized to body weight.

(catalog number DNOV030) EIA kits are 0.6 and 0.5 mIU/mL, respectively). The measured values were transformed to picograms per milliliter in the case of LH and FSH.

Statistical analysis

The results are shown as means ± SEM. Data were assessed for normality and homogeneity of variances by Kolgomorov-Smirnov tests and then analyzed by a one-way ANOVA (GraphPad Prism) followed by Bonferroni's or Tukey post hoc tests. In case of data showing non-Gaussian distribution, the Mann-Whitney *U* test was used. Body weight data were analyzed with a repeated-measure ANOVA, time being the repeated measure. In all cases, differences were considered statistically significant at $P < .05$.

Results

Vaginal opening: onset of puberty

Both ZEA and EE2 advanced puberty as measured by the number of rats showing vaginal opening, an external sign of puberty onset. One hundred percent of rats showed a vaginal opening at PND 24 or PND 25 in case of EE2- or ZEA-treated rats, respectively. None of the vehicle-treated control animals displayed a vaginal opening before the end of the experiment at PND 28 (Figure 1A). Vaginal opening in the naïve group occurred at PND 30–31 (Supplemental Figure 1). F1

Vaginal smears taken at the end of the experiment (PND 28) revealed that 62.5% of ZEA-treated rats showed proestrous-like, 12.5% estrous-like, and 25% metestrous-like smears. Among the rats treated with EE2 for 10 days, on the basis of vaginal smears, 37.5% were in proestrus, 37.5% in estrus, and 25% in metestrus.

Ten-day ZEA and EE2 treatment resulted in a significant enlargement of the uterus ($F_{[2.26]} = 35{,}10$, $P < .0001$) compared with controls. The normalized uterus weight of ZEA- or EE2-treated animals were 2.16-fold and 2.34-fold higher, respectively, than those of vehicle-treated rats (Figure 1B).

Histological analysis of the hematoxylin-eosin stained ovarian sections revealed a large number of small antral follicles in ZEA- and EE2-treated animals. No corpora lutea were observed in the xenoestrogen-treated rats (Supplemental Figure 2).

Because the timing of puberty depends on the metabolic resources of the animals, we checked whether xenoestrogen treatment affected body weight. Repeated-measures ANOVA on daily body weight data and one-way ANOVA on cumulative body weight gain data revealed a significant effect of treatment ($F_{[2.37]} = 10.58$, $P = .0002$). Bonferroni's post hoc test indicated that EE2-treated premature female rats gained significantly less body weight during the treatment period (PND 18–28) than vehicle- or ZEA-treated animals (Figure 2, A and B). Daily and cumulative food and water intake of the three groups were not significantly different (Supplemental Figure 3). F2

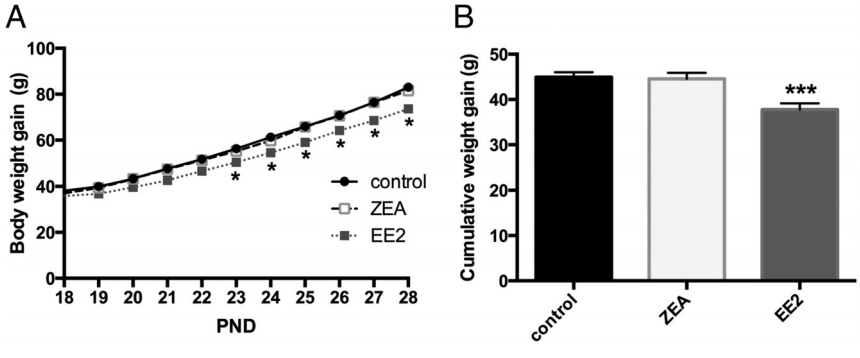

Figure 2. Effect of xenosestrogens on body weight. Mean ± SEM values of daily body weights (A) and cumulative weight gain (B) in vehicle-treated controls, ZEA- (10 mg/kg), and EE2 (10 μg/kg)-treated immature female rats are show (n = 38). The treatment started at PND18. ***, $P <$ 0,001.

Xenoestrogens increase *gnrh* expression in the hypothalamus

Next, we investigated the effect of xenoestrogens on *gnrh* mRNA levels in the hypothalamus. *gnrh* expression was significantly increased after EE2 or ZEA treatment as measured by a quantitative PCR from AVPV/POA-enriched brain tissues ($P = .0012$ for both xenoestrogens by a Mann-Whitney *U* nonparametric test) relative to vehicle-treated rats. ZEA and EE2 treatments resulted in 2.52-fold and 3.65-fold increases, respectively (Figure 3B). F3

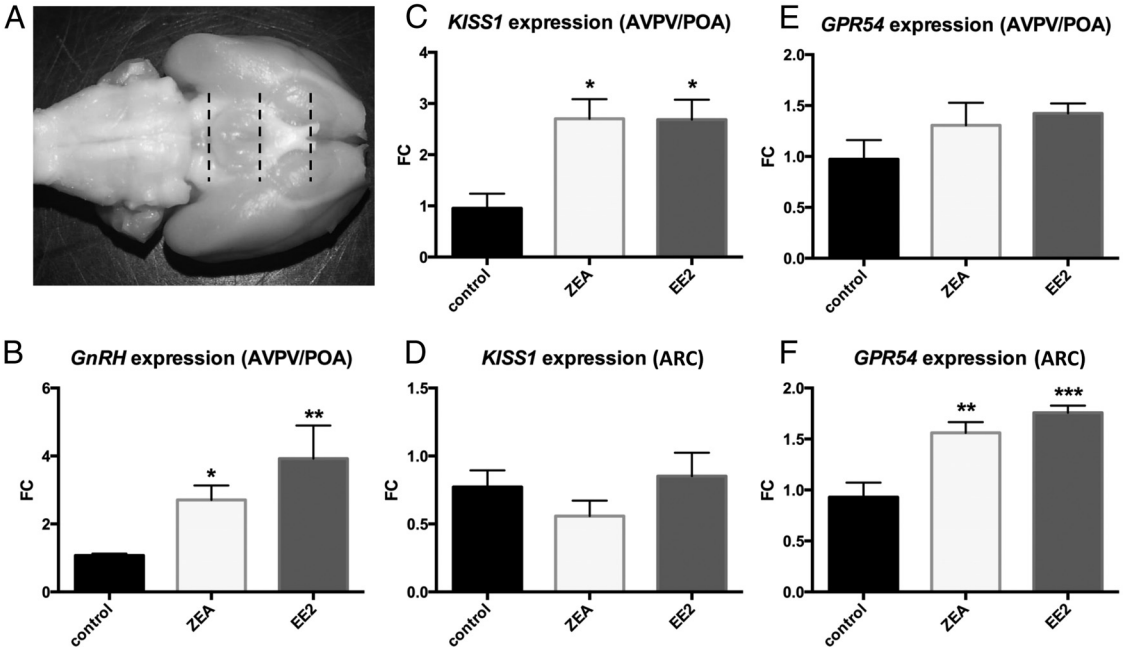

Figure 3. Effect of xenoestrogens on hypothalamic neuropeptide expression. A, Depiction of the cuts made to separate anterior and posterior hypothalamic blocks. B and C, Mean relative quantities of GnRH (*gnrh*) (B); KP (*kiss1*) (C and D) and KP receptor *gpr54* (E and F) mRNA in the anterior (AVPV/POA) (B, C, and E) and posterior (ARC) (D and F) hypothalamic blocks. FC, fold change compared with *gapdh*-normalized value of vehicle-treated rats. *, $P < .05$; **; $P < .01$; ***, $P < .0005$.

ZEA and EE2 differentially affect *kiss1* and *gpr54* mRNA levels in the hypothalamus

A peripubertal increase of *gnrh* is attributable, at least in part, to estrogen-sensitive inputs to the GnRH neurons. Among these, kisspeptinergic innervation plays a pivotal role in pubertal timing. Because *kiss1* expression is regulated reciprocally by estrogen in the AVPV/rostral periventricular (PeV) and ARC regions in the rodent brain, *kiss1* and kisspeptin receptor *gpr54* mRNA levels were measured in these brain areas separately. Both ZEA and EE2 treatment resulted in a significant increase in *kiss1* expression in the AVPV/PeV (ZEA: 2.83-fold increase; EE2: 2.82-fold increase), whereas in the ARC region, significant alterations were not observed (Figure 3, C and D). The expression of *gpr54* increased significantly only in the ARC (ZEA: 1.68-fold increase; EE2: 1.89-fold increase, Figure 3, E and F).

Within the arcuate block, the relative quantity of neurokinin B (*nkb*) mRNA levels decreased in ZEA- and EE2-treated rats ($F_{[2.11]} = 6.71$; $P = .013$). However, the expression of dynorphin (*dyn*) did not differ in xenoestrogen-treated animals compared with the vehicle-treated controls ($F_{[2.12]} = 0.17$; $P = .84$) (Figure 4). F4

No changes were detected in the hypothalamic mRNA levels of ERs *erα* ($F_{[2.10]} = 2.77$; $P = .11$) or *erβ* ($F_{[2.10]} = 1.27$; $P = .30$ not shown).

RING finger transcription factor makorin 3 (*mkrn3*) has been implicated in sexual development as a break of puberty (49). *Mkrn3* mRNA was elevated exclusively in the AVPV/PeV after the EE2 treatment (Supplemental Figure 4). A small increase in the mRNA level of *eed* was also detected in the anterior hypothalamic block (Supplemental Figure 4). The relative quantities of *cbx7*, *cux1*, *eap1*, and *ttf1* transcription factor mRNA remained unaltered in ZEA- and EE2-treated animals compared with vehicle controls (Supplemental Figures 5 and 6).

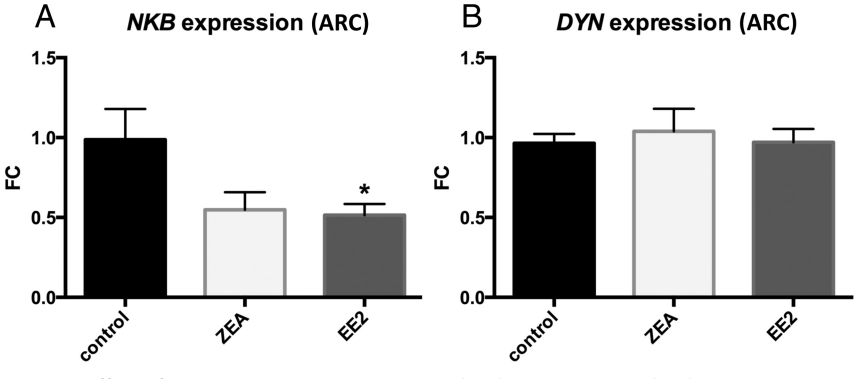

Figure 4. Effect of xenoestrogens on neurokinin B (*nkb*) and dynorphin (*dyn*) expression in the arcuate region. Fold change (mean ± SEM) values of ZEA- and EE2-treated animals compared with vehicle-treated controls are shown.

In situ hybridization histochemical localization of *kiss1 and gpr54* mRNA

In vehicle-treated female rats, we found *kiss1* in situ hybridization signals exclusively over the neurons in the AVPV, the rostral PeV, and the

AQ: 25

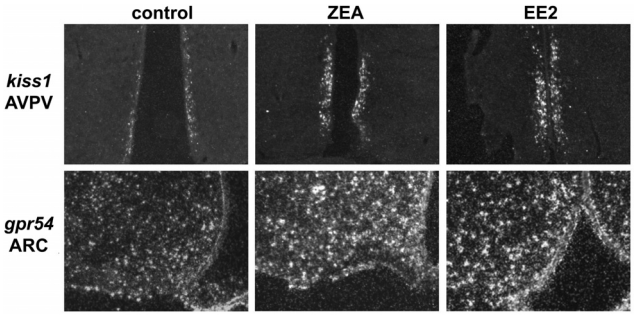

Figure 5. Effects of xenoestrogens on *kiss1* and *gpr54* mRNA signals in the hypothalamus. Representative dark-field autoradiograms showing signals obtained after in situ hybridization with cRNA probes. Top row, *kiss1* mRNA in the anterior periventricular region. Bottom row, *gpr54* mRNA signals in the ARC after the vehicle, ZEA, or EE2 treatments. Photomicrograph magnification, ×75.

ARC nuclei. In response to ZEA or EE2 administration, increased ~~KP~~ mRNA expression was revealed in the AVPV/PeV (Figure 5), without detectable changes in the ARC. Extrahypothalamic expression of *kiss1* was not detected after the xenoestrogen treatment. F5

^{35}S-uridine ~~5~~-triphosphate-labeled riboprobes corresponding to *gpr54* mRNA revealed a specific pattern of KP receptor expression in the rat brain. In vehicle-treated animals, intense hybridization signals were detected in the cortical layers as well as in the CA1–4 areas and the dentate gyrus of the hippocampal formation. Strong labeling corresponding to *gpr54* mRNA has been revealed in the lateral habenula, in the subfornical organ, bed nucleus of stria terminalis, and the mammillary region. Within the hypothalamus, the POA, suprachiasmatic, supraoptic, caudal paraventricular, ventromedial, and ARC nuclei were moderately labeled. In response to ZEA and EE2, there was a selective increase in the intensity of the hybridization signal in the medial basal hypothalamus (Figure 5). The strength and distribution of the hybridization signal at the extrahypothalamic areas also remained unchanged after ZEA and EE2 treatment (data not shown).

Endocrine disruptors increase KP fiber density in the preoptic area and the number of KP appositions onto GnRH neurons

Analysis of immunofluorescent material revealed an increased density of KP-immunoreactive fibers in the preoptic region of ZEA- and EE2-treated animals. One-way ANOVA revealed a significant treatment effect ($F_{[2.6]} = 5.65$, $P = .042$). Treatment with the endocrine disruptors resulted in 5-fold and 8-fold increases in the KP fiber density in the case of ZEA and EE2, respectively ($F_{[2.15]} = 12.06$, $P = .0008$) (Figure 6). F6

Furthermore, using double-labeled immunfluorescence, we revealed KP fibers in close apposition to GnRH neurons in the POA. Specifically, the number of KP appositions on GnRH neurons was significantly increased in

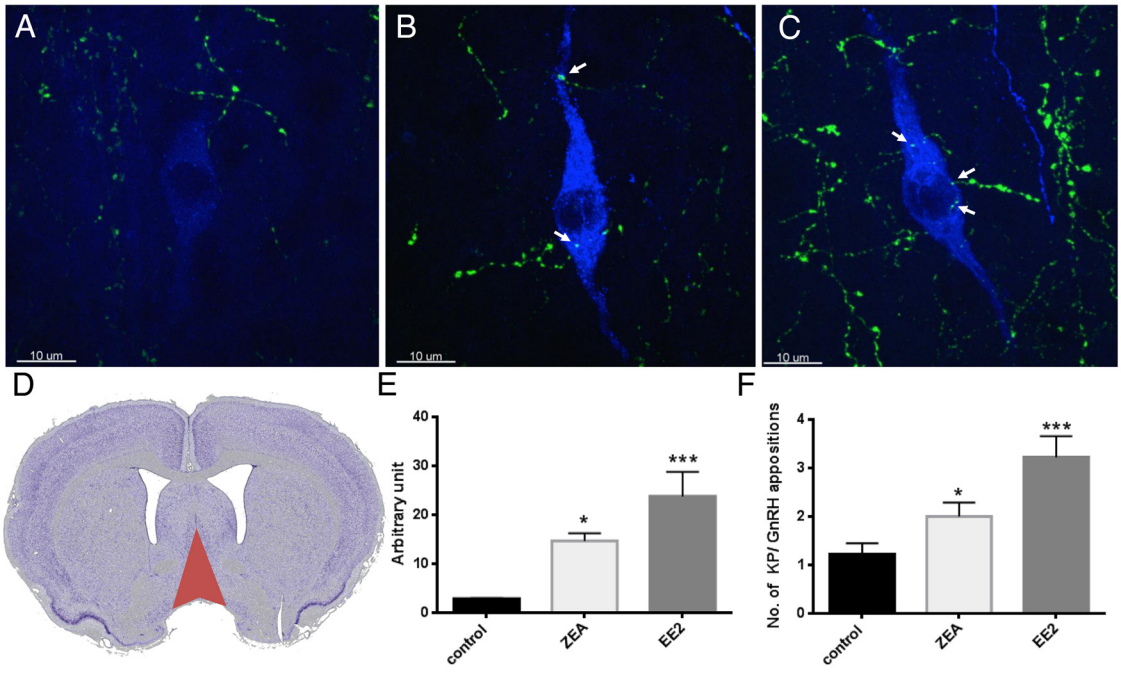

Figure 6. Changes in GnRH and kisspeptin immunostaining in the POA of xenoestrogen-treated prepubertal female rats. Top panels, Representative fluorescence images showing double labeling for GnRH (blue) and kisspeptin (green) in the POA of the vehicle-treated control (A), ZEA-treated (B), and EE2-treated (C) female rats. Bottom panels, Schematic drawing depicting the rostral POA as the region of interest for the quantitative analysis of KP-immunoreactive fibers (D). The density of the KP-immunoreactive fibers in the POA (E) and the number of kisspeptinergic profiles in close apposition with GnRH-immunoreactive neurons (F) in control, ZEA-, and EE2-treated female rats is shown.

COLOR

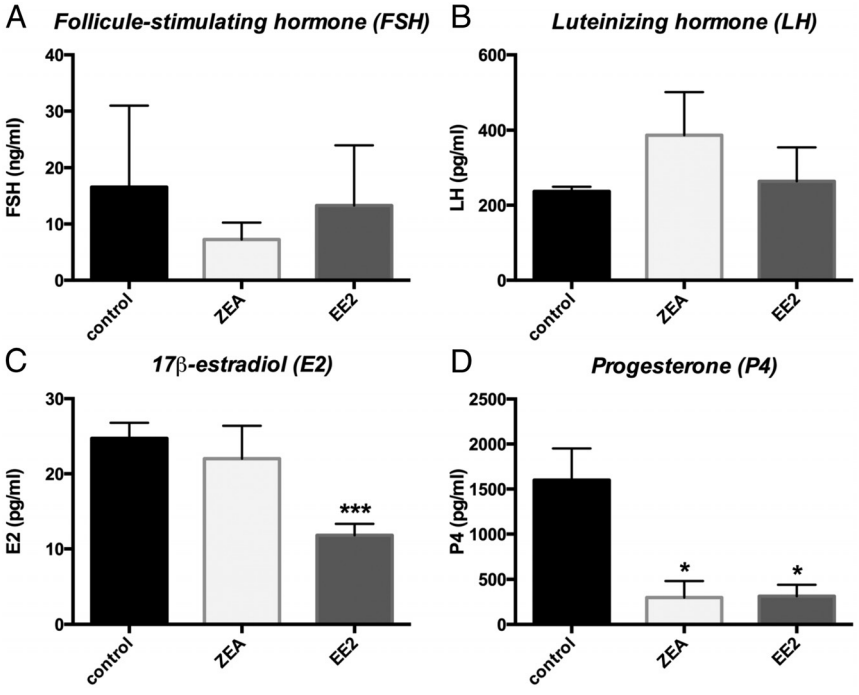

Figure 7. Plasma hormone levels after xenoestrogen treatment. Mean ± SEM values of plasma LH, FSH, and 17β-estradiol levels in vehicle- (control), ZEA-, and EE2-treated prepubertal rats (n = 10–12). **, $P < .01$.

AQ: 26

the EE2- and ZEA-treated animals ($F_{[2.24]} = 9.5$; $P = .0009$) (Figure 6).

Effect of ZEA on plasma hormone levels

Plasma LH ($F_{[2.11]} = 0.90$, $P = .42$) and FSH ($F_{[2.9]} = 0.14$, $P = .87$) concentrations did not change significantly after ZEA or EE2 treatment. EE2, but not ZEA, administration significantly reduced the 17β-estradiol concentration ($F_{[2.12]} = 8.01$, $P = .006$) by the end of the 10-day administration period (Figure 7).

F7

Discussion

This study shows that administration of two xenoestrogens, the synthetic estrogen derivative EE2 and the nonsteroidal mycoestrogen ZEA, to sexually immature prepubertal female rats advances puberty, which is paralleled by increases in KP signaling to GnRH neurons and increased *gnrh* expression. The effect of xenoestrogens on KP neurons is site and gene specific because 10 days of ZEA or EE2 administration elevated *kiss1* mRNA levels exclusively in the AVPV/PeV but not in the ARC region.

Previous experiments on laboratory rodents and domestic animals, and studies on mycotoxin exposed humans, have established the endocrine-disruptive and puberty-accelerating effects of ZEA. In this study on rats, we have used the time of vaginal opening as the first phenotypic marker of puberty onset in rodents, although the central and peripheral mechanisms that contribute to this process are not fully understood. It should also be noted that accelerated vaginal opening does not necessarily indicate onset of normal estrous cycles, and there are examples when the timing of vaginal opening and maturation of central neuroendocrine circuits are not correlated (50, 51). It is very likely that in addition to their central effects, xenoestrogens may directly stimulate peripheral estrogen-sensitive tissues such as the vagina and uterus to produce morphological and histological changes seen in puberty.

We found ZEA- and EE2-induced accelerated vaginal opening to be accompanied by significant increases in *gnrh* mRNA levels in the anterior hypothalamus. Indeed, stimulation of *gnrh* gene expression is the rate-limiting factor for the onset of puberty (52), although GnRH neurons are not directly responsive to the positive feedforward effects of estrogens that initiate sexual maturation.

Among the neurotransmitters and neuropeptides that regulate GnRH neurons, KPs and other RFamide-related peptides have been implicated in the mediation of estrogen effects and the progression of puberty. Most KP neurons express ERα (41, 48), and kisspeptinergic fibers have been identified to form synaptic contacts with GnRH neurons (53, 54) that possess GPR54, the KP receptor (29, 55). Furthermore, KP alters the electrophysiology and activation of GnRH neurons (56, 57). Sex steroids play a prominent role in driving morphological and functional plasticity of the hypothalamic KP system during puberty (40). During pubertal maturation, there is a significant increase in KP content and the number of contacts between KP and GnRH neurons (58). ZEA and EE2 elevated the KP fiber density in the anterior hypothalamus, and the number of KP appositions on GnRH neurons was also increased. Although these contacts have not been confirmed by high-resolution microscopy, the light microscopic morphological rearrangements seen after ZEA and EE2 administration are compatible with increased kisspeptinergic drive to GnRH neurons similar to that seen in normal puberty. During normal puberty, there is a shift from the inhibition to stimulation of GnRH neurons via changes in kisspeptinergic signaling. Based on our present data, ZEA and

doi: 10.1210/en.2015-1330

Table 1. Antibody Table

Peptide/ Protein Target	Antigen Sequence (If Known)	Name of Antibody	Manufacturer, Catalog Number, and/or Name of Individual Providing the Antibody	Species Raised (Monoclonal or Polyclonal)	Dilution Used
GnRH	Mammalian GnRH conjugated to bovine thyroglobulin	Guinea pig anti-GnRH	Erik Hrabovszky; number 1018	Guinea pig polyclonal	1:3000
Kisspeptin	Amino acids 43–52: YNWNSFGLRY (mouse)	Rabbit a-kisspeptin	Alain Caraty, number 566	rabbit polyclonal	1:10 000

EE2 stimulate GnRH expression via the activation of the AVPV KP drive. However, GnRH release and subsequent gonadotropin release is blocked by an excess of xenoestrogens.

One concern might be the specificity of the KP antibody because many of these antibodies cross-react with other members of RFRPs. Indeed, there are some mismatches between staining patterns generated by two N-terminal antibodies vs the C-terminal-specific antibody (AC566) used in this experiment (Table 1). However, KP staining remains after preabsorption with the RFRP antibody, whereas it is completely absent in KP knockout mice (59).

In addition to morphological changes in kisspeptinergic neurocircuits, we have revealed a significant increase in the *kiss1* mRNA levels in the hypothalamus after 10 days' administration of endocrine disruptor compounds. Of note, our data revealed site-specific effects of ZEA and EE2 on kisspeptin expression in the AVPV region, which is compatible with the positive feedback effect of estrogens on KP synthesis in this region. An estrogen-mediated gradual increase of KP peptide expression is necessary for puberty onset (60). It is intriguing that ZEA or EE2 treatment in the prepubertal period had no effect on *kiss1* mRNA levels in the arcuate nucleus.

The molecular mechanisms through which estrogenic compounds produce opposite effects on *kiss1* transcription at AVPV and ARC remain to be fully explored. Previous studies indicated that estrogen-induced *kiss1* expression in the AVPV requires an ER-DNA interaction, whereas the inhibition of KP mRNA levels in the ARC occurs through a nongenomic action or other ERE-independent effects of estrogens. ZEA and EE2 might also increase *kiss1* transcription in the AVPV through the classical nuclear estrogen-response element-mediated pathway. In support of this, it has been shown ~~in vitro~~ that ZEA had strong estrogenic effects due to its ability to activate both activation function-1 and activation function-2 functions (61).

As yet, the potential contribution of such differential signaling to the developmental actions of xenoestrogens has not been studied in detail and will merit specific investigation. This differential regulatory pathway may explain the different sensitivity of KP neurons to the normal organizing effects of sex steroids in different hypothalamic nuclei; AVPV neurons display a higher degree of sexual dimorphism than ARC neurons in rodents (30). In addition, recognition of this divergent regulatory mechanism may help to define the different modes of actions of estrogens and xenoestrogens on KP neurons, which may involve nonclassical ER pathways as well as ER-independent mechanisms, in line with emerging data in other target tissues of endocrine disruptors. It should be added, however, that long-term treatment with ZEA or EE2 did not alter ERα/ERβ mRNA levels in the hypothalamus. Another possibility for the differential effect of these xenoestrogens on KP neuron populations would be differential recruitment of steroid receptor coactivators or corepressors in the AVPV vs ARC.

Two critical periods have been identified during the sexual development in which rodents are specifically vulnerable to endogenous and exogenous estrogenic compounds including endocrine disruptors: the perinatal and the peripubertal age (62). Prenatal, neonatal, or early postnatal exposure of natural, synthetic, or phyto/xenoestrogens can have both feminizing and defeminizing effects on the developing neural mechanisms that control sexual behavior (63). KP neurons are especially sensitive to both the early organizing and the acute regulatory actions of estrogens (62). These organizational steroid actions cause reduced kisspeptin transcription and cell numbers in the AVPV and KP inputs to GnRH neurons in adults. For instance, female rats exposed in utero (gestational d 6–21) to EE2 were heavier and had delayed vaginal opening, aberrant estrous cyclicity, and masculinized behavior (64). By contrast, upon exposure during the prepubertal, activation phase, estrogens stimulate *kiss1* mRNA and KP fiber density in the hypothalamus and drive GnRH neurons. Here we have provided evidence that the estrogenic mycotoxin ZEA and EE2 administered to female rats at prepubertal ages increases *kiss1* expression, enhances the density of KP-immunoreactive fibers in the anterior hypothalamus, and increases appositions between KP-containing profiles and GnRH neurons similarly to changes seen during puberty. These transcriptional changes and

morphological rearrangements might be responsible for the enhanced *gnrh* mRNA transcription and puberty acceleration. Our data on the prepubertal effects of EE2 are in contrast with data obtained by Overgaard et al (65), who found a minor if any effect of perinatal EE2 exposure on hypothalamic kisspeptin expression or puberty onset. From birth to puberty, there is a continuous increase in the number of KP-neurons in the AVPV region (58), and KP action through GPR54 on GnRH neurons are essential for triggering HPG activity. Our present study confirmed ~~GPR54~~ expression in the hypothalamus. However, mRNA levels after ZEA and EE2 treatment did not change in the preoptic region, whereas it increased in the ARC.

The timing of puberty onset is genetically encoded, epigenetically modified, influenced by stimulatory and restraining factors, and is very sensitive to metabolic and environmental cues. ~~RING~~ finger transcription factor makorin 3 (MKRN 3) has recently been identified as a major developmental restraining factor of the GnRH pulse generator (43, 66). In mice, expression of *mkrn3* mRNA in the ARC is highest at PND 10–12 and its gradual decline correlates with the increase of *Kiss1* and *Tac2* at puberty onset (43). Two genes (*eed* and *cbx7*) of the Polycomb group of the transcriptional silencing complex (67) have also been recently implicated in the inhibitory control of hypothalamic *kiss1* expression and puberty (42). Because neither *mkrn3* nor *eed* and *cbx7* mRNA levels decrease in response to xenoestrogens, it is likely that EE2 and ZEA advance puberty by stimulating propuberty factors rather than by inhibiting puberty restraining mechanisms.

Puberty timing depends on the metabolic status, which is conferred by hormonal inputs (such as leptin) that signal the energy supplies of the body (68, 69). It is not likely, however, that ZEA and EE2 significantly affect this pathway because these compounds did not result in overt increase of white fat depots. By contrast, EE2 treatment significantly reduced body weight gain, similar to that observed in ovariectomized rodents after estrogen treatment (70).

AQ: 20

One other confounding factor would be the stress associated with the oral gavage, which has recently been show to alter organization of the ERα circuit in the limbic system (71) and might interact with the effects of EE2 or ZEA. However, stress in general~~ly~~, and stress-induced CRH in particular, delay, rather than accelerate, puberty, as seen in xenoestrogen-treated rats.

Exposure to other endocrine disruptors, such as bisphenol A, genistein, diethylstilbestrol, and dichlorodiphenyl-trichloroethane, also affect the timing of the vaginal opening, depending on the critical age window (for review see reference 72). Furthermore, some estrogenic ~~1-ethyl-3-(3-dimethylaminopropyl)-carbodiimides~~ alter HPG regulation through the kisspeptinergic system. For instance, it has been very recently shown that the acute administration of bisphenol A at proestrus to adult female mice enhances positive estrogenic action and results in an increase of KP activity and *gnrh* expression (73). By contrast, in testing of EE2 and an extensive array of pesticides and their combination throughout gestation and lactation, Overgaard et al (65) did not find a significant effect on *kiss1* expression.

AQ: 21

AQ: 22

The xenoestrogen doses used in our experiments have relevance for human exposure. The dose of EE2 corresponds to a daily intake of contraceptive pills taken by adolescent girls for birth control or for treatment of hypogonadism.

The risk of ZEA exposure is increasing: according to a recent analysis, 93%–96% of cereal samples have been contaminated by ZEA in northern Europe (74). The levels vary by country and by year, but so far, the highest ZEA concentration, 49 mg/kg, was found in a wheat sample from Australia (75). In a retrospective analysis of girls involved in a school epidemic of premature thelarche in Northern Italy, elevated serum zearalenone/zeranol concentrations were detected (23).

It should also be noted, however, that our data have a number of limitations in comparison with human exposure. We have used relatively high doses of xenoestrogens and gave them for a limited time at a postnatal/peripubertal age. By contrast, the population is exposed to several compounds at low levels but sometimes for much more prolonged (even life-long) time periods. Furthermore, it is increasingly recognized that the effect of xenoestrogens might be additive with other endocrine disruptive compounds. These complex interactions warrant further studies.

In summary, our present data show that exposure of peripubertal rats to the structurally different xenoestrogens EE2 and ZEA advances puberty onset, very likely by increasing/amplifying the kisspeptinergic drive to GnRH neurons. Because of the high probability of exposure to xenoestrogens, one might be aware of the possible endocrine disruptive effects of these compounds especially in the peripubertal life period.

Acknowledgments

AQ:23–24

We thank Professor György Buzsáki and Dr Mark D. Eyre for reading the manuscript.

Address all correspondence and requests for reprints to: Krisztina J. Kovács, PhD, Laboratory of Molecular Neuroendocrinology, Institute of Experimental Medicine, Szigony utca 43, Budapest H-1083, Hungary. E-mail: kovacs@koki.hu.

This work was supported by Grants 109622 (to K.J.K.), 109744 (to S.F.), 101326 (to I.K.), and K112669 (to E.H.) from the Hungarian Research Fund.

Disclosure Summary: The authors have nothing to disclose.

References

1. **Zinedine A, Soriano JM, Molto JC, Manes J.** Review on the toxicity, occurrence, metabolism, detoxification, regulations and intake of zearalenone: an oestrogenic mycotoxin. *Food Chem Toxicol*. 2007; 45:1–18.
2. **Kuiper-Goodman T, Scott PM, Watanabe H.** Risk assessment of the mycotoxin zearalenone. *Regul Toxicol Pharmacol*. 1987;7:253–306.
3. **European Food Safety Authority.** Scientific opinion on the risks for public health related to the presence of zearalenone in food. *EFSA J*. 2011;9:1–22.
4. **Takemura H, Shim JY, Sayama K, Tsubura A, Zhu BT, Shimoi K.** Characterization of the estrogenic activities of zearalenone and zeranol in vivo and in vitro. *J Steroid Biochem Mol Biol*. 2007;103: 170–177.
5. **Cozzini P, Dellafiora L.** In silico approach to evaluate molecular interaction between mycotoxins and the estrogen receptors ligand binding domain: a case study on zearalenone and its metabolites. *Toxicol Lett*. 2012;214:81–85.
6. **Bovee TF, Helsdingen RJ, Rietjens IM, Keijer J, Hoogenboom RL.** Rapid yeast estrogen bioassays stably expressing human estrogen receptors α and β, and green fluorescent protein: a comparison of different compounds with both receptor types. *J Steroid Biochem Mol Biol*. 2004;91:99–109.
7. **Heneweer M, Houtman R, Poortman J, Groot M, Maliepaard C, Peijnenburg A.** Estrogenic effects in the immature rat uterus after dietary exposure to ethinylestradiol and zearalenone using a systems biology approach. *Toxicol Sci*. 2007;99:303–314.
8. **Kriszt R, Krifaton C, Szoboszlay S, et al.** A new zearalenone biodegradation strategy using non-pathogenic *Rhodococcus pyridinivorans* K408 strain. *PLoS One*. 2012;7:e43608.
9. **Kiang DT, Kennedy BJ, Pathre SV, Mirocha CJ.** Binding characteristics of zearalenone analogs to estrogen receptors. *Cancer Res*. 1978;38:3611–3615.
10. **Mueller SO, Simon S, Chae K, Metzler M, Korach KS.** Phytoestrogens and their human metabolites show distinct agonistic and antagonistic properties on estrogen receptor α (ERα) and ERβ in human cells. *Toxicol Sci*. 2004;80:14–25.
11. **Cortinovis C, Pizzo F, Spicer LJ, Caloni F.** Fusarium mycotoxins: effects on reproductive function in domestic animals—a review. *Theriogenology*. 2013;80:557–564.
12. **Etienne M, Jemmali M.** Effects of zearalenone (F2) on estrous activity and reproduction in gilts. *J Anim Sci*. 1982;55:1–10.
13. **Zhao F, Li R, Xiao S, et al.** Postweaning exposure to dietary zearalenone, a mycotoxin, promotes premature onset of puberty and disrupts early pregnancy events in female mice. *Toxicol Sci*. 2013;132: 431–442.
14. **Long GG, Turek J, Diekman MA, Scheidt AB.** Effect of zearalenone on days 7 to 10 post-mating on blastocyst development and endometrial morphology in sows. *Vet Pathol*. 1992;29:60–67.
15. **Nikaido Y, Danbara N, Tsujita-Kyutoku M, Yuri T, Uehara N, Tsubura A.** Effects of prepubertal exposure to xenoestrogen on development of estrogen target organs in female CD-1 mice. *In Vivo*. 2005;19:487–494.
16. **Edwards S, Cantley TC, Day BN.** The effects of zearalenone on reproduction in swine. II. The effect on puberty attainment and postweaning rebreeding performance. *Theriogenology*. 1987;28: 51–58.
17. **Fara GM, Del Corvo G, Bernuzzi S, et al.** Epidemic of breast enlargement in an Italian school. *Lancet*. 1979;2:295–297.
18. **Comas AP.** Precocious sexual development in Puerto Rico. *Lancet*. 1982;1:1299–1300.
19. **Schoental R.** Precocious sexual development in Puerto Rico and oestrogenic mycotoxins (zearalenone). *Lancet*. 1983;1:537.
20. **Szuts P, Mesterhazy A, Falkay G, Bartok T.** Early telarche symptoms in children and their relations to zearalenon contamination in foodstuffs. *Cereal Res Commun*. 1997;25:429–436.
21. **Combalbert S, Hernandez-Raquet G.** Occurrence, fate, and biodegradation of estrogens in sewage and manure. *Appl Microbiol Biotechnol*. 2010;86:1671–1692.
22. **Aris AZ, Shamsuddin AS, Praveena SM.** Occurrence of 17α-ethynylestradiol (EE2) in the environment and effect on exposed biota: a review. *Environ Int*. 2014;69:104–119.
23. **Massart F, Meucci V, Saggese G, Soldani G.** High growth rate of girls with precocious puberty exposed to estrogenic mycotoxins. *J Pediatr*. 2008;152:690–695, 695.e691.
24. **Katzenellenbogen JA, O'Malley BW, Katzenellenbogen BS.** Tripartite steroid hormone receptor pharmacology: interaction with multiple effector sites as a basis for the cell- and promoter-specific action of these hormones. *Mol Endocrinol*. 1996;10:119–131.
25. **Watanabe H, Suzuki A, Kobayashi M, Lubahn DB, Handa H, Iguchi T.** Similarities and differences in uterine gene expression patterns caused by treatment with physiological and non-physiological estrogens. *J Mol Endocrinol*. 2003;31:487–497.
26. **Lee JH, Miele ME, Hicks DJ, et al.** KiSS-1, a novel human malignant melanoma metastasis-suppressor gene. *J Natl Cancer Inst*. 1996; 88:1731–1737.
27. **Gottsch ML, Cunningham MJ, Smith JT, et al.** A role for kisspeptins in the regulation of gonadotropin secretion in the mouse. *Endocrinology*. 2004;145:4073–4077.
28. **Han SK, Gottsch ML, Lee KJ, et al.** Activation of gonadotropin-releasing hormone neurons by kisspeptin as a neuroendocrine switch for the onset of puberty. *J Neurosci*. 2005;25:11349–11356.
29. **Shahab M, Mastronardi C, Seminara SB, Crowley WF, Ojeda SR, Plant TM.** Increased hypothalamic GPR54 signaling: a potential mechanism for initiation of puberty in primates. *Proc Natl Acad Sci USA*. 2005;102:2129–2134.
30. **Clarkson J, Herbison AE.** Postnatal development of kisspeptin neurons in mouse hypothalamus: sexual dimorphism and projections to gonadotropin-releasing hormone neurons. *Endocrinology*. 2006; 147:5817–5825.
31. **Gottsch ML, Navarro VM, Zhao Z, et al.** Regulation of Kiss1 and dynorphin gene expression in the murine brain by classical and nonclassical estrogen receptor pathways. *J Neurosci*. 2009;29:9390–9395.
32. **Seminara SB, Messager S, Chatzidaki EE, et al.** The GPR54 gene as a regulator of puberty. *N Engl J Med*. 2003;349:1614–1627.
33. **Semple RK, Achermann JC, Ellery J, et al.** Two novel missense mutations in g protein-coupled receptor 54 in a patient with hypogonadotropic hypogonadism. *J Clin Endocrinol Metab*. 2005;90: 1849–1855.
34. **Kirilov M, Clarkson J, Liu X, et al.** Dependence of fertility on kisspeptin-Gpr54 signaling at the GnRH neuron. *Nat Commun*. 2013; 4:2492.
35. **Novaira HJ, Sonko ML, Hoffman G, et al.** Disrupted kisspeptin signaling in GnRH neurons leads to hypogonadotrophic hypogonadism. *Mol Endocrinol*. 2014;28:225–238.
36. **Xu Y, Nedungadi TP, Zhu L, et al.** Distinct hypothalamic neurons mediate estrogenic effects on energy homeostasis and reproduction. *Cell Metab*. 2011;14:453–465.
37. **Yeo SH, Clarkson J, Herbison AE.** Kisspeptin-gpr54 signaling at the GnRH neuron is necessary for negative feedback regulation of luteinizing hormone secretion in female mice. *Neuroendocrinology*. 2014;100:191–197.
38. **Dubois SL, Acosta-Martinez M, DeJoseph MR, et al.** Positive, but not negative feedback actions of estradiol in adult female mice re-

quire estrogen receptor α in kisspeptin neurons. *Endocrinology*. 2015;156:1111–1120.

39. **Smith JT, Cunningham MJ, Rissman EF, Clifton DK, Steiner RA.** Regulation of Kiss1 gene expression in the brain of the female mouse. *Endocrinology*. 2005;146:3686–3692.
40. **Garcia-Galiano D, Pinilla L, Tena-Sempere M.** Sex steroids and the control of the Kiss1 system: developmental roles and major regulatory actions. *J Neuroendocrinol*. 2012;24:22–33.
41. **Mayer C, Acosta-Martinez M, Dubois SL, et al.** Timing and completion of puberty in female mice depend on estrogen receptor α-signaling in kisspeptin neurons. *Proc Natl Acad Sci USA*. 2010;107:22693–22698.
42. **Lomniczi A, Loche A, Castellano JM, et al.** Epigenetic control of female puberty. *Nat Neurosci*. 2013;16:281–289.
43. **Abreu AP, Dauber A, Macedo DB, et al** Central precocious puberty caused by mutations in the imprinted gene MKRN3. *N Engl J Med*. 2013;368:2467–2475.
44. **Durmaz E, Asci A, Erkekoglu P, Akcurin S, Gumusel BK, Bircan I.** Urinary bisphenol a levels in girls with idiopathic central precocious puberty. *J Clin Res Pediatr Endocrinol*. 2014;6:16–21.
45. **Chen CY, Chou YY, Wu YM, Lin CC, Lin SJ, Lee CC.** Phthalates may promote female puberty by increasing kisspeptin activity. *Hum Reprod*. 2013;28:2765–2773.
46. **Simmons DM, Arriza JL, Swanson LW.** A complete protocol for in situ hybridization of messenger RNAs in brain and other tissues with radiolabeled single-stranded RNA probes. *J Histotechnol*. 1989;12:169–181.
47. **Hrabovszky E, Molnar CS, Sipos MT, et al.** Sexual dimorphism of kisspeptin and neurokinin B immunoreactive neurons in the infundibular nucleus of aged men and women. *Front Endocrinol (Lausanne)*. 2011;2:80.
48. **Franceschini I, Lomet D, Cateau M, Delsol G, Tillet Y, Caraty A.** Kisspeptin immunoreactive cells of the ovine preoptic area and arcuate nucleus co-express estrogen receptor α. *Neurosci Lett*. 2006;401:225–230.
49. **Macedo DB, Abreu AP, Reis AC, et al.** Central precocious puberty that appears to be sporadic caused by paternally inherited mutations in the imprinted gene makorin ring finger 3. *J Clin Endocrinol Metab*. 2014;99:E1097–E1103.
50. **Bateman HL, Patisaul HB.** Disrupted female reproductive physiology following neonatal exposure to phytoestrogens or estrogen specific ligands is associated with decreased GnRH activation and kisspeptin fiber density in the hypothalamus. *Neurotoxicology*. 2008;29:988–997.
51. **Franssen D, Ioannou YS, Alvarez-Real A, et al.** Pubertal timing after neonatal diethylstilbestrol exposure in female rats: neuroendocrine vs peripheral effects and additive role of prenatal food restriction. *Reprod Toxicol*. 2013;44:63–72.
52. **Gore AC, Wu TJ, Rosenberg JJ, Roberts JL.** Gonadotropin-releasing hormone and NMDA receptor gene expression and colocalization change during puberty in female rats. *J Neurosci*. 1996;16:5281–5289.
53. **d'Anglemont de Tassigny X, Fagg LA, Carlton MB, Colledge WH.** Kisspeptin can stimulate gonadotropin-releasing hormone (GnRH) release by a direct action at GnRH nerve terminals. *Endocrinology*. 2008;149:3926–3932.
54. **Clarkson J, Han SK, Liu X, Lee K, Herbison AE.** Neurobiological mechanisms underlying kisspeptin activation of gonadotropin-releasing hormone (GnRH) neurons at puberty. *Mol Cell Endocrinol*. 2010;324:45–50.
55. **Messager S, Chatzidaki EE, Ma D, et al.** Kisspeptin directly stimulates gonadotropin-releasing hormone release via G protein-coupled receptor 54. *Proc Natl Acad Sci USA*. 2005;102:1761–1766.
56. **Clarkson J, d'Anglemont de Tassigny X, Moreno AS, Colledge WH, Herbison AE.** Kisspeptin-GPR54 signaling is essential for preovulatory gonadotropin-releasing hormone neuron activation and the luteinizing hormone surge. *J Neurosci*. 2008;28:8691–8697.
57. **Liu X, Lee K, Herbison AE.** Kisspeptin excites gonadotropin-releasing hormone neurons through a phospholipase C/calcium-dependent pathway regulating multiple ion channels. *Endocrinology*. 2008;149:4605–4614.
58. **Clarkson J.** Effects of estradiol on kisspeptin neurons during puberty. *Front Neuroendocrinol*. 2013;34:120–131.
59. **Clarkson J, d'Anglemont de Tassigny X, Colledge WH, Caraty A, Herbison AE.** Distribution of kisspeptin neurones in the adult female mouse brain. *J Neuroendocrinol*. 2009;21:673–682.
60. **Clarkson J, Boon WC, Simpson ER, Herbison AE.** Postnatal development of an estradiol-kisspeptin positive feedback mechanism implicated in puberty onset. *Endocrinology*. 2009;150:3214–3220.
61. **Li Y, Burns KA, Arao Y, Luh CJ, Korach KS.** Differential estrogenic actions of endocrine-disrupting chemicals bisphenol A, bisphenol AF, and zearalenone through estrogen receptor α and β in vitro. *Environ Health Perspect*. 2012;120:1029–1035.
62. **Brock O, Bakker J.** The two kisspeptin neuronal populations are differentially organized and activated by estradiol in mice. *Endocrinology*. 2013;154:2739–2749.
63. **Bakker J, Baum MJ.** Role for estradiol in female-typical brain and behavioral sexual differentiation. *Front Neuroendocrinol*. 2008;29:1–16.
64. **Ferguson SA, Law CD, Kissling GE.** Developmental treatment with ethinyl estradiol, but not bisphenol A, causes alterations in sexually dimorphic behaviors in male and female Sprague Dawley rats. *Toxicol Sci*. 2014;140:374–392.
65. **Overgaard A, Holst K, Mandrup KR, et al.** The effect of perinatal exposure to ethinyl oestradiol or a mixture of endocrine disrupting pesticides on kisspeptin neurons in the rat hypothalamus. *Neurotoxicology*. 2013;37:154–162.
66. **de Vries L, Gat-Yablonski G, Dror N, Singer A, Phillip M.** A novel MKRN3 missense mutation causing familial precocious puberty. *Hum Reprod*. 2014;29:2838–2843.
67. **Simon JA, Kingston RE.** Mechanisms of polycomb gene silencing: knowns and unknowns. *Nat Rev Mol Cell Biol*. 2009;10:697–708.
68. **Castellano JM, Bentsen AH, Mikkelsen JD, Tena-Sempere M.** Kisspeptins: bridging energy homeostasis and reproduction. *Brain Res*. 2010;1364:129–138.
69. **Castellano JM, Tena-Sempere M.** Metabolic regulation of kisspeptin. *Adv Exp Med Biol*. 2013;784:363–383.
70. **Gao Q, Horvath TL.** Cross-talk between estrogen and leptin signaling in the hypothalamus. *American J Physiol Endocrinol Metab*. 2008;294:E817–E826.
71. **Cao J, Rebuli ME, Rogers J, et al.** Prenatal bisphenol A exposure alters sex-specific estrogen receptor expression in the neonatal rat hypothalamus and amygdala. *Toxicol Sci*. 2013;133:157–173.
72. **Parent AS, Franssen D, Fudvoye J, Gerard A, Bourguignon JP.** Developmental variations in environmental influences including endocrine disruptors on pubertal timing and neuroendocrine control: revision of human observations and mechanistic insight from rodents. *Front Neuroendocrinol*. 2015;38:12–36.
73. **Wang X, Chang F, Bai Y, Chen F, Zhang J, Chen L.** Bisphenol A enhances kisspeptin neurons in anteroventral periventricular nucleus of female mice. *J Endocrinol*. 2014;221:201–213.
74. **Uhlig S, Eriksen GS, Hofgaard IS, Krska R, Beltran E, Sulyok M.** Faces of a changing climate: semi-quantitative multi-mycotoxin analysis of grain grown in exceptional climatic conditions in Norway. *Toxins (Basel)*. 2013;5:1682–1697.
75. **Rodrigues I, Naehrer K.** A three-year survey on the worldwide occurrence of mycotoxins in feedstuffs and feed. *Toxins (Basel)*. 2012;4:663–675.